PHARMACIA

Pharmacia 70(4): 887–894
DOI 10.3897/pharmacia.70.e109898

Research Article

In vitro antimitotic activity and *in silico* study of some 6-fluoro-triazolo-benzothiazole analogues

Naresh Podila[1], Mithun Rudrapal[1], Subramanyam Sibbala[1], Atul R. Bendale[2], Yanadaiah Palakurthi[3], Molakpogu Ravindra Babu [3], Kiran Manda[4], Renzon Daniel Cosme Pecho[5], Sreelatha Muddisetti[6]

1 *Department of Pharmaceutical Sciences, School of Biotechnology and Pharmaceutical Sciences, Vignan's Foundation for Science, Technology & Research, Vadlamudi, Guntur-522213, Andhra Pradesh, India*
2 *Mahabir Institute of Pharmacy, Nashik-422004, Maharashtra, India*
3 *School of Pharmaceutical Sciences, Lovely Professional University, Phagwara-144001, Punjab, India*
4 *Department of Pharmaceutical Chemistry, Shri Vishnu College of Pharmacy, Bhimavaram-534202, Andhra Pradesh, India*
5 *Department of Chemistry, Universidad San Ignacio de Loyola, La Molina-1524, Lima, Peru*
6 *Vikas College of Pharmaceutical Sciences, Suryapet-508376, Andhra Pradesh, India*

Corresponding author: Naresh Podila (nareshtrcp10@gmail.com)

Received 21 July 2023 ♦ **Accepted** 2 August 2023 ♦ **Published** 28 September 2023

Citation: Podila N, Rudrapal M, Sibbala S, Bendale AR, Palakurthi Y, Babu MR, Manda K, Pecho RDC, Muddisett S (2023) *In vitro* antimitotic activity and *in silico* study of some 6-fluoro-triazolo-benzothiazole analogues. Pharmacia 70(4): 887–894. https://doi.org/10.3897/pharmacia.70.e109898

Abstract

In this work, nine 6-fluoro-triazolo-benzothiazole derivatives were prepared and evaluated for *in vitro* antimitotic activity. In addition, *in silico* study was also done using tubulin protein (PDB: 6QQN) by molecular docking method. Results revealed that TZ2 and TZ9 were the most active compounds with antimitotic action opposing the standard drug, aspirin. Results of molecular docking exhibited the inhibitory potential of triazolo-benzothiazole against tubulin protein. The mitotic study indicates the efficacy of triazolo-benzothiazole analogues in inhibiting the proliferation of cancer cells either by promoting microtubule formation or affecting microtubules, thereby preventing microtubule breakdown.

Keywords

Benzothiazole, 1,2,4-triazole, cancer, antimitotic activity, aspirin, mung beans

Introduction

Cancer is a major cause of mortality globally, in both industrialized and developing nations (Mollinedo and Gajate 2003). Many synthetic and natural anticancer medications cure various forms of leukaemias, lymphomas, and solid tumours. Despite great advances in cancer chemotherapy, the management of cancer is still a challenging task. Over the past decades, various highly active natural and synthetic compounds with anticancer potential have been discovered, including microtubule poisons such as paclitaxel and other taxanes, which have proved beneficial in treating certain cancers like breast cancer, lung cancer, and ovarian cancer.

Benzothiazole is an interesting moiety in medicinal chemistry that has been reported to exhibit anticancer, an-

titumor, antimicrobial, anticonvulsant, anti-diabetic, antitubercular, and antibacterial activity (Siddiqui et al. 2007; Rajeeva et al. 2009; Dewangan et al. 2010; Nitin et al. 2010; Naresh et al. 2013; Sharma et al. 2013; Prabhu et al. 2015; Naresh et al. 2021). The second position of the benzothiazole moiety is suitable for substitution. The benzothiazole moiety fused with triazole ring with halogen substitutions of the phenyl ring could be an ideal scaffold for the development of therapeutic agents against cancer and other infectious diseases (bacterial, fungal and tubercular). In this work, some novel 6-fluoro-triazolo-benzothiazole analogues were designed and synthesized for their evaluation as antimitotic agents (Fig. 1). To identify potential tubulin inhibitors *in silico* study of the designed analogues was also carried out by molecular docking method.

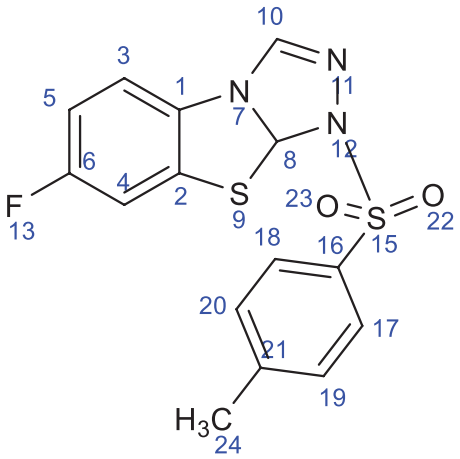

Figure 1. 6-fluoro-triazolo-benzothiazole scaffold.

Materials and methods

All the chemicals used were of synthetic grade. The melting point was determined by digital melting point apparatus. Thin-layer chromatography (TLC) was used to monitor the progress of reaction progress by using GF_{254} precoated aluminum plates (Merck), ethyl acetate: n-hexane (3:1) as the mobile phase, and ultra-violet (UV) chamber for visualization of spots. ELICIO FT-IR spectrometer was used to acquire the IR spectrum (Annavarapu et al. 2022). The ^{1}H-NMR spectra were recorded in deuterated dimethyl sulfoxide (DMSO-d_6) using a BRUKER Av 400 spectrometer. Using Shimadzu GC-MS QP 5000, mass spectra (MS) were recorded.

Chemistry

Synthesis of 7-chloro-6-fluorobenzo[d]thiazol-2-amine

About 1.45 g (0.01 mole) of fluorochloro aniline and 8 gm (0.08 mole) of potassium thiocyanate were mixed with 20 mL of cold glacial acetic acid and 1.6 mL of bromine solution was added into it from a dropping funnel and agitated with a magnetic stirrer in an ice bath. The mixture was agitated for 10 hours at room temperature after adding the bromine solution. Overnight, an orange precipitate was formed at the bottom of the flask, it was then added with 6 mL of water and the mixture was promptly heated to 85 °C and filtered. The reaction mixture was cooled and neutralized which finally yielded a dark brown precipitate. After benzene re-crystallization and animal charcoal treatment, 2-amino-6-fluoro-7-chloro-(1,3)-benzothiazole was obtained as green precipitate (1 gm, 51.02%, melted at 210–212 °C) after drying in 80 °C in an oven.

Synthesis of 7-chloro-6-fluoro-2-hydrazinyl-benzo[d]thiazole

To a 500 mL round bottom flask, 10 mL of concentrated HCl was added drop wise to 12 mL (0.02 mole) of hydrazine hydrate while stirring at 5–10 °C. After cooling the solution, 20.2 gm of 7-chloro-6-fluoro 2-amino benzothiazole was added, followed by 60 mL of ethylene glycol. The resulting mixture was refluxed for 3 hours processed by first letting the residue sink to the bottom of a beaker filled with crushed ice, then filtering, drying, and recrystallizing with ethanol.

Synthesis of 8-chloro-7-fluoro-1,9a-dihydrol [1,2,4] triazole [3,4-b][1,3] benzothiazole

About 2.19 gm of 7-chloro-6-fluoro-2-hydrazinyl-1,3-benzothiazole and 1 gm of potassium carbonate were added to 25 mL of formic acid in a 250 mL round bottom flask. The adduct was stabilized after two hours of refluxing in crushed ice. The residue was then purified and dried to obtain the pure product.

Synthesis of 8-chloro-7-fluoro-1-[4-methylphenyl]sulphonyl-1,9a-dihydro[1,2,4]triazolo[3,4-b][1,3]benzothiazole

In a 500 mL of round bottom flask, 2.2 gm of 8-chloro-7-fluoro-1,9a-dihydrol [1,2,4] triazole (0.013 mole) was transferred in the presence of pyridine and 1.71 g of *p*-toluene sulphonamide, (0.02 mole) after which it was refluxed for two hours, poured onto pulverized ice, drained, final purified residue was obtained by recrystallization with ethanol.

In a 100 mL round bottom flask, 2.7 gm of 8-chloro-7-fluoro-1-[4-methylphenylsulphonyl-1,9a-dihydro [1,2,4] triazolo [3,4b] [1,3] *benzothiazole* was refluxed with equal quantities of primary and secondary aromatic amines for 2 hours in DMF. The mélange was chilled before being spread over pulverised ice. Using a sprinkle of activated charcoal, after alcohol and benzene separation, the material was filtered, dehydrated, and recrystallized from alcohol. The scheme of synthesis of 6-fluoro-triazolo-benzothiazole analogues is depicted in Fig. 2.

6-fluoro-3-[(4-methylphenyl) sulfonyl]-N-(2-amino phenylamino)-3,3a-dihydro [1,2,4] triazolo [5,1-b][1,3] benzothiazol-5-amine (TZ1): Yield: 83%; white powder; mp: 112–114 °C; mf: $C_{21}H_{18}FN_5O_2S_2$, mw: 455.52; R_f = 0.74 (EtOAc: n-But: $CHCl_3$ 2:1:1); FT-IR (KBr, cm^{-1}): 1276.78, 1432.75, 1660, 1069, 1442, 1105, 1196; ^{1}H-NMR (DMSO-d_6, 300 MHz) δ ppm: 6.78–6.86 (m, 11H, Ar) 4.28 (s, 1H, NH_2) 3.01 (m, 3H, CH_3), 8.50 (s, 1H, NH); ^{13}C-NMR ($CDCl_3$, 100

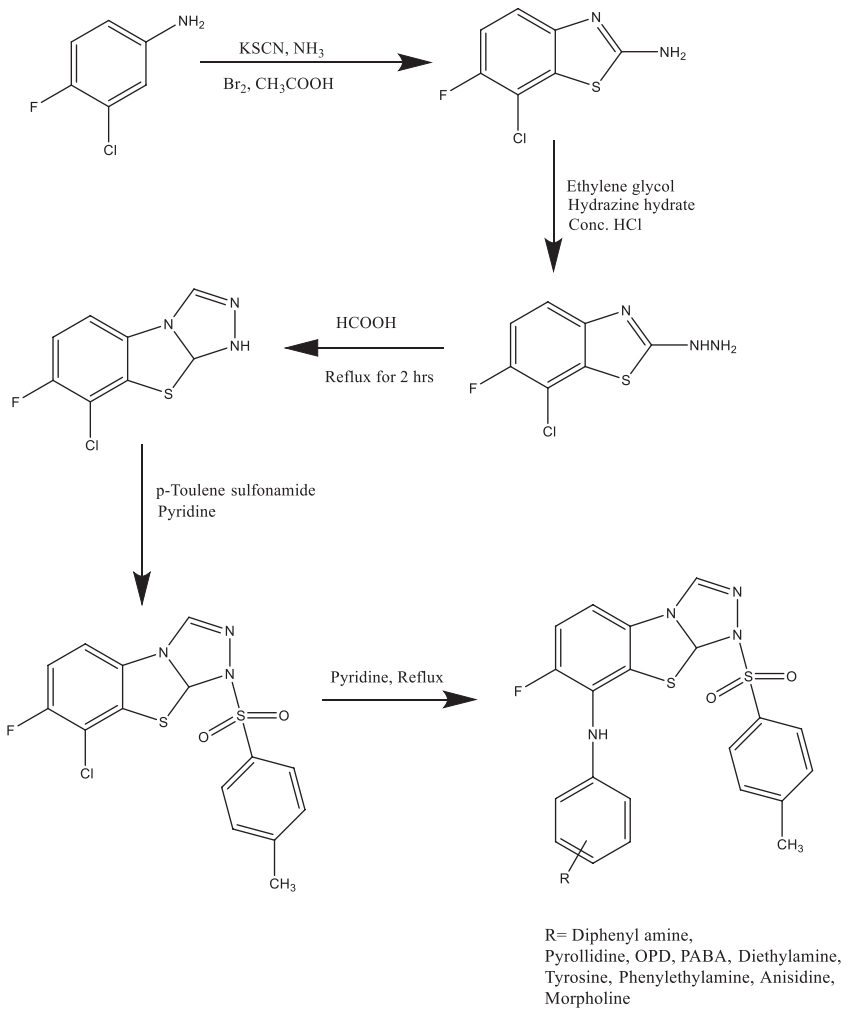

Figure 2. Scheme of synthesis for 6-fluoro-triazolo-benzothiazole analogues.

MHz) δ ppm: 24.3, 59.5, 104.8, 110.2, 113.5, 117.2, 119.1, 119.7, 119.9, 122.8, 127.2, 127.8, 129.2, 129.4, 129.8, 133.2, 136.7, 138.4, 141.5, 149.1, 154.8; MS (m/z), M^+: 455.50.

6-fluoro-3-[(4-methylphenyl)sulfonyl]-N-(4-hydroxy-propanoic acid)-3,3a-dihydro [1,2,4] triazolo [5,1-b] [1,3] benzothiazol-5-amine (TZ2): Yield: 49%; Brown solid; mp: 118–122 °C; mf: $C_{24}H_{21}FN_4O_5S_2$; mw: 528.57; R_f = 0.69 (EtOAc: n-Bu: $CHCl_3$: 2:1:1); FT-IR (KBr, cm^{-1}): 1348.45, 1527.14, 1598.48, 1127.34, 1398.72, 1164.64, 1118.53; ^{1}H-NMR (DMSO-d_6, 300 MHz) δ ppm: 6.21–6.92 (m, 10H, Ar) 9.38 (s, 1H, NH), 1.96 (m, 3H, CH_3) 2.98 (s, 2H, CH_2), 9.81, 13.10 (d, 2H, OH); ^{13}C-NMR ($CDCl_3$, 100 MHz) δ ppm: 24.8, 35.5, 60.8, 65.9, 67.4, 82.7, 103.7, 104.8, 113.6, 114.8, 115.3, 128.1, 129.4, 129.6, 129.8, 132.2, 133.4, 133.8, 136.5, 141.4, 143.2, 154.0, 155.6, 174.2 MS (m/z), M^+: 528.24.

N-(carboxy phenyl amino)-6-fluoro-3-[(4-methyl phenyl) sulfonyl]-3,3a-dihydro [1,2,4] triazole [5,1-b] [1,3] benzothiazol-5-amine (TZ3): Yield: 72.8%; orange solid; mp: 161–163 °C; mf: $C_{21}H_{17}FN_4O_3S_2$; mw: 456.41; R_f = 0.70 ($CHCl_3$: n-Bu: EtOAc: 1:2:1); FT-IR (KBr, cm^{-1}): 1298.21, 1521.57, 1614.57, 1152.86, 1487.45, 1019.26, 1224.26; ^{1}H-NMR (DMSO-d_6, 300 MHz) δ ppm: 7.16–7.23 (m, 8H, Ar), 9.38 (s, 1H, NH), 2.15 (m, 3H, CH_3) 2.99 (s, 2H, CH_2), 9.87, 11.82 (d, 2H, OH), 3.14 (s, 1H, NH); ^{13}C-NMR ($CDCl_3$, 100 MHz) δ ppm: 24.6, 60.2, 104.2, 110.5, 113.4, 116.2, 116.8, 120.2, 120.6, 127.2, 127.6, 129.1, 129.4, 129.7, 133.3. 136.5, 141.6, 148.2, 149.1, 154.3, 162.6; MS (m/z), M^+: 456.15.

N-(4-methoxyphenylamino)-6-fluoro-3-[(4-methyl phenyl) sulfonyl]-3,3a-dihydro [1,2,4] triazolo [5,1-b] [1,3] benzothiazol-5-amine (TZ4): Yield: 48.6%; pink solid; mp: 186–188 °C; mf: $C_{22}H_{19}FN_4O_3S_2$; mw: 470.53; R_f = 0.53 ($CHCl_3$: n-But: EtOAc: 2:1:1); FT-IR (KBr, cm^{-1}): 1311.85, 1538.47, 1597.41, 1123.82, 1476.14, 1083.53, 1191.68; ^{1}H-NMR (DMSO-d_6, 300 MHz) δ ppm: 7.12 -7.68 (m, 10H, Ar), 9.31 (s, 1H, NH), 3.01 (m, 3H, CH_3), 2.92 (s, 2H, CH_2), 3.27, 2.45 (s, 2H, CH_2); ^{13}C-NMR ($CDCl_3$, 100 MHz) δ ppm: 24.2, 55.9, 60.4, 104.8, 110.3, 113.6, 115.2, 115.6, 120.1, 120.8, 127.2, 127.4, 129.3, 129.6, 129.9, 131.9, 133.6, 141.6, 149.5, 150.2, 152.4, 154.6; MS (m/z), M^+: 470.25.

6-fluoro-3-[(4-methylphenyl)sulfonyl]-morpho-nyl-3,3a-dihydro [1,2,4] triazolo [5,1-b] [1,3] benzothi-azol-5-amine (TZ5): Yield: 63.14%, milkfish; mp: 168–172 °C; mf: $C_{19}H_{20}FN_5O_3S_2$; mw: 449.51; R_f = 0.82 (EtOAc:n-Bu1: $CHCl_3$: 2:1:1); FT-IR (KBr, cm^{-1}): 1198.57, 1457.01, 1668.27, 1125.65, 1502.48, 1183.34, 1210.01; ^{1}H-NMR (DMSO-d_6,

300 MHz) δ ppm: 7.15–7.83 (m, 5H, Ar), 1.98 (m, 3H, CH_3) 3.18 (s, 2H, CH_2), 3.01–3.47 (m, 4H, CH_2); ^{13}C-NMR ($CDCl_3$, 100 MHz) δ ppm: 24.6, 41.7, 56.1, 56.3, 60.4, 64.2, 64.5, 104.5, 105.7, 113.4, 127.2, 127.7, 128.4, 129.4, 129.9, 132.6, 136.6, 141.8, 143.2; MS (m/z), M^+: 449.32.

6-fluoro-(4-pyrrolidinyl)-3-[(4-methylphenyl)sulphonyl]-3,3a-dihydro [1,2,4]triazolo [5,1-b] [1,3] benzthiazol-5-amine (TZ6): Yield: 51.5%; cream; mp: 176–178 °C; mf: $C_{19}H_{19}FN_4O_2S_2$; mw: 418.50; R_f = 0.87 (EtOAc: n-But:$CHCl_3$ 2:1:1); FT-IR (KBr, cm^{-1}): 1301.20, 1558.51, 1637.68, 1084.45, 1493.29, 1137.87, 1204.60; ^{1}H-NMR (DMSO-d_6, 300 MHz) δ ppm: 6.78–6.85 (m, 6H, Ar), 3.00 (m, 3H, CH_3) 1.99 (m, 2H, CH_2), 2.96–3.47 (m, 4H, CH_2); ^{13}C-NMR ($CDCl_3$, 100 MHz) δ ppm: 24.6, 25.2, 25.5, 51.2, 51.8, 60.4, 104.7, 104.8, 105.4, 112.3, 126.3, 126.9, 127.8, 129.3, 129.8, 132.5, 136.2, 140.5, 142.4; MS (m/z), M^+: 418.27.

6-fluoro-N-diethylamino-3-[(4-methylphenyl)sulfonyl]-3,3a-dihydro [1,2,4] triazolo [5,1-b] [1,3] benzothiazol-5-amine (TZ7): Yield: 63.7%, blue; mp: 110–112 °C; mf: $C_{19}H_{21}FN_4O_2S_2$; mw: 420.52; R_f = 0.52 (EtOAc : n-But: $CHCl_3$ 2:1:1); FT-IR (KBr, cm^{-1}): 1310.21, 1522.57, 1685.01, 1107.27, 1524.84, 1098.21, 1267.47; ^{1}H-NMR (DMSO-d_6, 300 MHz) δ ppm: 7.04 -7.34 (m, 5H, Ar), 2.04 - 3.64 (m, 6H, CH_3) 2.97 (m, 4H, CH_2); ^{13}C-NMR ($CDCl_3$, 100 MHz) δ ppm: 24.15, 43.1, 52.3, 54.8, 61.2, 64.8, 64.9, 101.3, 104.3, 112.6, 123.4, 127.4, 128.3, 128.7, 129.4, 131.2, 133.8, 141.8, 144.9; MS (m/z), M^+: 420.12.

1-[6-fluoro-7-(4-phenethyl amino)-3-[4-methyl phenyl] sulphonyl]-3,3a dihydro [1, 2, 4] triazole [5,1-b] [1,3] benzothiazole (TZ8): Yield: 57.9%; green; mp: 116–119 °C; mf: $C_{23}H_{21}FN_4O_2S_2$; mw: 468.56; R_f = 0.72 (EtOAc: n-Bu1: $CHCl_3$: 2:1:1); FT-IR (KBr, cm^{-1}): 1317.34, 1503.04, 1621.27, 1089.57, 1457.14, 1200.62, 1243.18; ^{1}H-NMR (DMSO-d_6, 300 MHz) δ ppm: 7.07–7.64 (m, 11H, Ar), 3.05–3.83 (m, 4H, CH_2) 7.68 (s, H, NH) 3.08 (m, 3H, CH_3); ^{13}C-NMR ($CDCl_3$, 100 MHz) δ ppm: 23.4, 25.3, 44.8, 53.6, 60.8, 62.7, 69.4, 103.5, 106.7, 110.2, 114.6, 124.6, 127.6, 128.9, 129.1, 129.6, 129.8, 130.4, 132.7, 134.8, 1412.3, 144.6, 148.3; MS (m/z), M^+: 468.25.

6-fluoro-3-[(4-methyl phenyl) sulfonyl]-5-(naphthyl amino)-3,3a-dihydro[1,2,4] triazolo [5,1- b] [1,3] Benzothiazole (TZ9): Yield:63.78%; violet; mp: 155–158 °C; mf: $C_{25}H_{19}FN_4O_2S_2$; mw: 490.57; R_f = 0.91 (EtOAc: n-Bul:$CHCl_3$: 2:1:1); FT-IR (KBr, cm^{-1}): 1314.47, 1582.17, 1605.23, 1041.89, 1487.24, 1317.27, 1151.07; ^{1}H-NMR (DMSO-d_6, 300 MHz) δ ppm: 7.13–7.82 (m, 6H, aromatic), 3.14–3.57 (m, 4H, CH_2) 9.27 (s, 4H, NH) 2.37 (m, 3H, CH_3); ^{13}C-NMR ($CDCl_3$, 100 MHz) δ ppm: 21.3, 23.5, 26.4, 27.6, 40.6, 45.7, 61.2, 64.3, 84.5, 102.3, 108.4, 110.8, 116.2, 125.3, 126.4, 126.8, 128.6, 128.9, 129.5, 130.2, 130.6, 130.9, 131.2, 133.4, 1491.57; MS (m/z), M^+: 490.30.

Evaluation of antimitotic activity

The antimitotic activity was evaluated according to a previously reported method (Raheel et al. 2017). For six hours, the average weight of mung beans was steeped in the standard, control, and test solutions. The solution was drained after six hours and the radical, which is 1.0–1.5 cm long was measured. Mass, radical length and seed germination were recorded.

Molecular docking

Molecular docking was performed on PyRx 0.8 platform (Ghosh et al. 2021; Junejo et al. 2021; James et al. 2022; Archana et al. 2023; Celik et al. 2023; Devasia et al. 2023). PyRx determines ligand-protein binding affinity in molecular docking (Rudrapal et al. 2022a; Rudrapal et al. 2022b; Rudrapal et al. 2022c; Rudrapal et al. 2022d; Rudrapal et al. 2022e; Zothantluanga et al. 2022; Rudra-

Table 1. Antimitotic data of synthesized compounds.

Sl. No.	Compound code	Name of drug and concentration	Initial weight (gms)	Weight at		Drain radical length		No. of seeds germinated		% seeds germinated	
				T_o (gm)	T_{48} (gm)	T_o(cm)	T_{48} (cm)	T_o	T_{48}	T_o	T_{48}
1	TZ1	1 mg	1.52	2.63	3.89	1.29	1.38	9	11	50%	60%
		3 mg	1.54	3.17	4.21	1.19	1.30	12	14	55%	65%
2.	TZ2	1 mg	1.56	3.21	4.52	1.12	1.25	11	12	50%	65%
		3 mg	1.54	3.52	4.12	0.81	1.06	12	13	55%	60%
3.	TZ3	1 mg	1.52	3.12	4.21	1.00	1.12	7	9	35%	45%
		3 mg	1.54	2.25	3.74	0.89	1.21	9	11	40%	45%
4.	TZ4	1 mg	1.54	3.09	3.99	0.78	0.84	9	11	50%	60%
		3 mg	1.55	3.13	3.89	0.52	0.72	10	12	55%	65%
5.	TZ5	1 mg	1.55	3.48	3.85	0.69	0.89	9	10	50%	65%
		3 mg	1.56	3.24	3.98	0.71	0.74	10	11	55%	60%
6.	TZ6	1 mg	1.54	2.48	3.61	0.72	0.79	9	10	50%	55%
		3 mg	1.52	3.04	3.94	0.74	0.82	10	11	40%	55%
7.	TZ7	1 mg	1.55	3.34	4.18	0.89	1.14	9	10	40%	50%
		3 mg	1.54	3.42	3.99	0.86	0.83	10	11	40%	55%
8.	TZ8	1 mg	1.52	3.45	3.75	0.89	0.86	8	10	45%	55%
		3 mg	1.55	3.51	3.81	0.85	0.94	9	11	40%	55%
9.	TZ9	1 mg	1.52	2.73	3.93	1.32	1.45	10	12	50%	60%
		3 mg	1.54	3.07	4.02	1.25	1.32	11	13	55%	65%
10.	Standard	1 mg	1.56	3.64	4.32	0.52	0.58	7	9	35%	45%
	Aspirin	3 mg	1.54	3.42	4.12	0.58	0.62	6	8	30%	40%
11.	Control		1.56	3.52	4.32	1.05	0.98	9	11	45%	55%

pal et al. 2023). Tubulin protein (PDB: 6QQN) was used at a resolution of 1.50 Å. The size of grid box was 0.3750 Å. The 200 step MMFF94 force field with an RMS gradient of 0.1 was used for the study. The protein's binding site (grid box) was chosen first to perform docking (Othman et al. 2021; Kumar et al. 2022; Kumar et al. 2023; Pasala et al. 2022a; Pasala et al. 2022b; Rashid et al. 2022; Issahaku et al. 2023; Paul et al. 2023). All synthesized ligands were docked in the active site of the protein molecule. The PyRx score classified all ligands by binding affinity. The ligands were categorized by their binding energies.

Results and discussion

Chemistry

Fig. 2 shows the synthetic strategy of 6-fluoro triazolo-benzothiazole derivatives (TZ1–TZ9). The final compounds are derivatives of 8-chloro-7-fluoro-1-[4-methylphenyl]sulphonyl-1,9a-dihydro[1,2,4]triazolo[3,4-b][1,3] benzothiazole. As presented in the experimental section, FT-IR, ^{1}H-NMR, and MS data supported the structure of synthesized compounds.

Antimitotic activity

Anti-mitotic activity was tested for all the compounds (TZ1–TZ9) (Table 1). Aspirin was used as standard compound at 1 and 3 mg/mL. Results revealed that TZ2 and TZ9 were the most active opposing the standard drug. TZ1, TZ7, and TZ4 also exhibited appreciable activity. *In vitro* anticancer drug screening requires antimitotic action. In the present study, the mitotic index of 6-fluoro triazolo-benzothiazole analogues indicates the efficacy of compounds in inhibiting the proliferation of cancer cells either by promoting microtubule formation or affecting microtubules, thereby preventing microtubule breakdown. This causes the cells to become so congested with microtubules that they can no longer divide and develop. As a result, cells stop dividing and eventually perish via apoptosis.

Docking assessment

The three-dimensional structure of tubulin and guanosine triphosphate (PDB: 6QQN) was used in the study. Prior to docking active site amino acid residues were identified. The following amino acids viz., Gln146, Thr145, Gln11, Ser178, Ala180, Asn101, Asp98, Glu71, Ser140, Gln144, Gln143, Ala100, ASP69, Tyr224, Ser140, and Ala99 are present in the catalytic pocket of the protein molecule, as shown in Fig. 3. Ramachandran map verified the protein, as represented in Fig. 4.

PyRx calculated binding energies of protein-ligand complexes. The protein-ligand interaction is a measure of binding affinity. The binding affinity of TZ9 (-10.9 kcal/mol) was the highest among the selected molecules whose binding energy was greater than that of standard aspirin

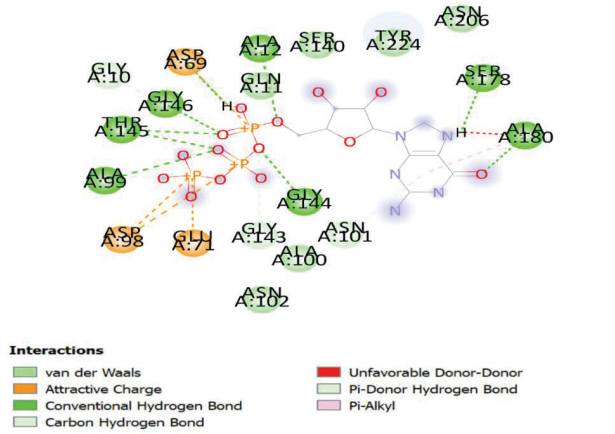

Figure 3. Amino acids present in the active site of the catalytic pocket of the tubulin receptor (PDB id: 6QQN).

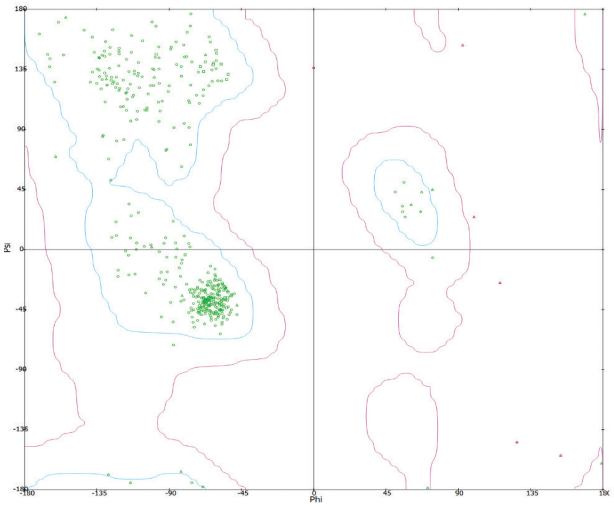

Figure 4. Ramachandran plot of tubulin receptor (PDB id: 6QQN).

(-6.5 kcal/mol) and co-crystal ligand (guanosine triphosphate) (-8.2 kcal/mol). Table 2 presents two dimensional (2D) interactions between ligands (TZ1–TZ9) and 6QQN. Fig. 5a–d displays two dimensional (2D) interactions between TZ2 and 6QQN, TZ9 with 6QQN, aspirin and 6QQN, and guanosine triphosphate with 6QQN.

Conclusion

In this work, nine 6- fluoro-triazolo-benzothiazole derivatives were prepared and evaluated for *in vitro* antimitotic activity. In addition, *in silico* study was also done using tubulin protein (PDB: 6QQN) by molecular docking method. The antimitotic study indicates the efficacy of triazolo-benzothiazole analogues in inhibiting the proliferation of cancer cells either by promoting microtubule formation or affecting microtubules, thereby preventing microtubule breakdown.

Conflict of interest

The authors declare no conflict of interest.

Table 2. Compounds and their binding energies.

Sl. No.	Compound code	Binding energy (kcal/mole)	No. of hydrogen bonds	Ligand group	Interacting amino acid residue
1	TZ1	-9.7	4	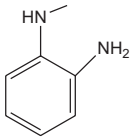	Ser178, Gln77, Ser140, Gln11
2	TZ2	-9.8	4	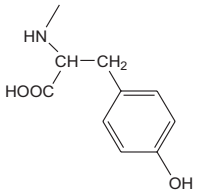	Asp69, Gln11, Ser140, Ser178
3	TZ3	-8.7	3	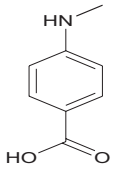	Tyr224, Glu22, Ala19
4	TZ4	-8.3	3	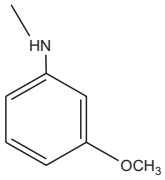	Ser140, Tyr224, Ser178
5	TZ5	-8.5	2	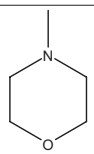	Val177, Ser140
6	TZ6	-8.7	1	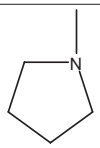	Ser140
7	TZ7	-7.9	2	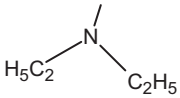	Arg229, Gln15
8	TZ8	-8.4	3	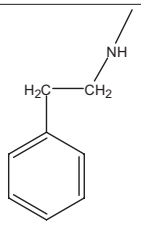	Thr82, Glu77, Gln15
9	TZ9	-10.1	4	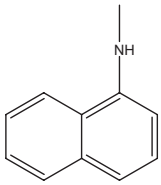	Ala12, Gln11, Ser140, Asn101
10	Aspirin	-6.5	1	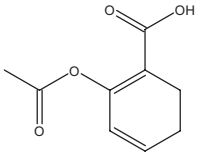	Asn206

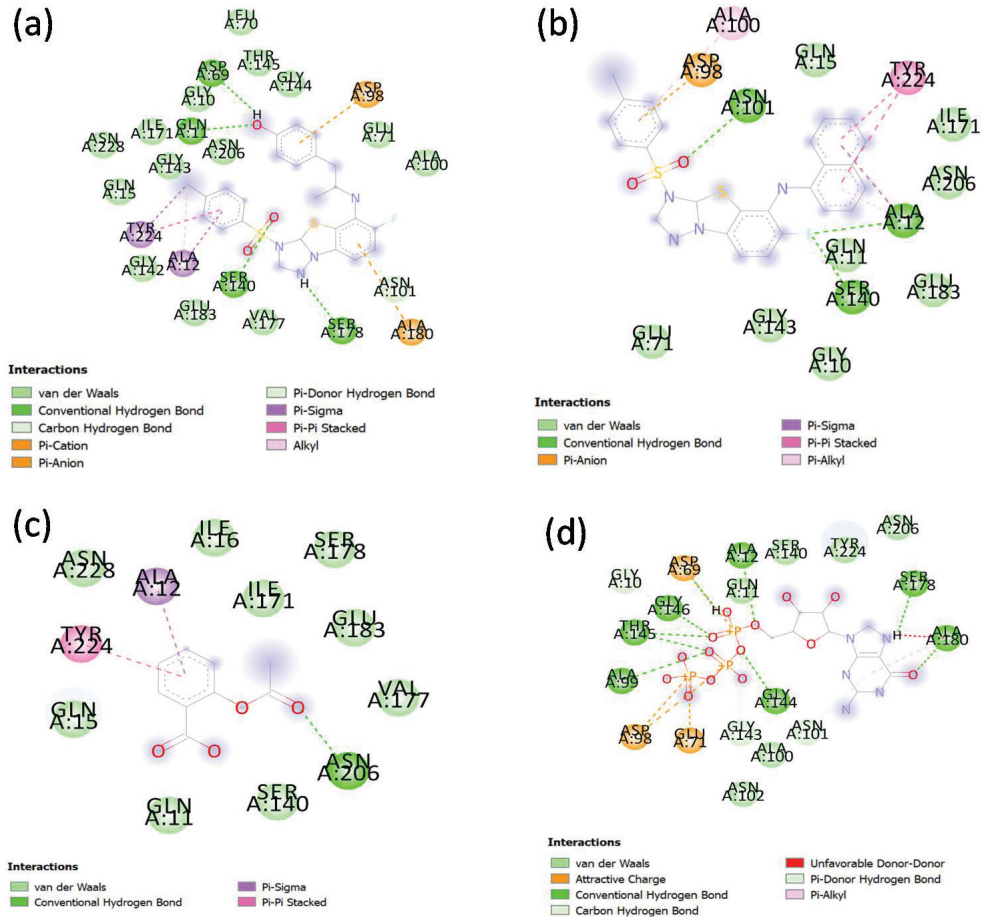

Figure 5. **(a)** 2D interaction of TZ2 on 6QQN, **(b)** 2D interaction of TZ9 on 6QQN, **(c)** 2D interaction of aspirin on 6QQN, and **(d)** 2D interaction of guanosine triphosphate on 6QQN.

References

Annavarapu TR, Kamepalli S, Konidala SK, Kotra V, Challa SR, Rudrapal M, Bendale AR (2022) Antioxidant and anti-inflammatory activities of 4-allylpyrocatechol and its derivatives with molecular docking and ADMET investigations. Bulletin of University of Karaganda-Chemistry 105(1): 50–59. https://doi.org/10.31489/2022Ch1/50-59

Archana VP, Armaković SJ, Armaković S, Celik I, Bhagyasree JB, Dinesh Babu KV, Rudrapal M, Divya IS, Pillai RR (2023) Exploring the structural, photophysical and optoelectronic properties of a diaryl heptanoid curcumin derivative and identification as a SARS-CoV-2 inhibitor. Journal of Molecular Structure 1281: 135110. https://doi.org/10.1016/j.molstruc.2023.135110

Celik I, Rudrapal M, Yadalam PK, Chinnam S, Balaji TM, Varadarajan S, Khan J, Patil S, Walode SG, Panke DV (2023a) Resveratrol and its natural analogues inhibit RNA dependant RNA polymerase (RdRp) of *Rhizopus oryzae* in mucormycosis through computational investigations. Polycyclic Aromatic Compounds 43(5): 4426–4443. https://doi.org/10.1080/10406638.2022.2091618

Devasia J, Chinnam S, Khatana K, Shakya S, Joy F, Rudrapal M, Nizam A (2023) Synthesis, DFT, and in silico anti-COVID evaluation of novel tetrazole analogues. Polycyclic Aromatic Compounds 43(3): 1941–1956. https://doi.org/10.1080/10406638.2022.2036778

Dewangan D, Pandey A, Sivakumar T, Rajavel R, Dubey RD (2010) Synthesis of some novel 2, 5-disubstituted 1, 3, 4-oxadiazole and its analgesic, anti-inflammatory, anti-bacterial and anti-tubercular activity. International Journal of Chem Tech Research 2(3): 1397–1412.

Ghosh S, Chetia D, Gogoi N, Rudrapal M (2021) Design, molecular docking, drug-likeness and molecular dynamics studies of 1,2,4-trioxane derivatives as novel *Plasmodium falciparum* falcipain-2 (FP-2) inhibitors. Biotechnologia 102(3): 257–275. https://doi.org/10.5114/bta.2021.108722

James AE, Okoro UC, Ezeokonkwo MA, Bhimapaka CR, Rudrapal M, Ugwu DI, Gogoi N, Chetia D, Celik I (2022) Design, synthesis, molecular docking, molecular dynamics and *in vivo* antimalarial activity of new dipeptide-sulfonamides. ChemistrySelect 7(5): e202103908. https://doi.org/10.1002/slct.202103908

Junejo JA, Zaman K, Rudrapal M, Celik I, Attah EI (2021) Antidiabetic bioactive compounds from *Tetrastigma angustifolia* (Roxb.) Deb and *Oxalis debilis* Kunth.: Validation of ethnomedicinal claim by *in vitro* and *in silico* studies. South African Journal Botany 143: 164–173. https://doi.org/10.1016/j.sajb.2021.07.023

Kumar Pasala P, Donakonda M, Dintakurthi PS, Rudrapal M, Gouru SA, Ruksana K (2023) Investigation of cardioprotective activity of silybin: Network pharmacology, molecular docking, and *in vivo* studies. ChemistrySelect 8(20): e202300148. https://doi.org/10.1002/slct.202300148

Kumar PP, Shaik RA, Khan J, Alaidarous MA, Rudrapal M, Khairnar SJ, Sahoo R, Zothantluanga JH, Walode SG (2022) Cerebroprotective effect of Aloe Emodin: *in silico* and *in vivo* studies. Saudi Journal of Biological Sciences 29: 998–1005. https://doi.org/10.1016/j.sjbs.2021.09.077

Othman IMM, Mahross MH, Gad-Elkareem MAM, Rudrapal M, Gogoi N, Chetia D, Aouadi K, Snoussi M, Kadri A (2021) Toward a treatment of antibacterial and antifungal infections: Design, synthesis and in vitro activity of novel arylhydrazothiazolylsulphonamide analogues and their insight of DFT, docking and molecular dynamics simulations. Journal of Molecular Structure 1243: 130862. https://doi.org/10.1016/j.molstruc.2021.130862

Pasala PK, Siva Reddy SSL, Silvia N, Reddy DY, Sampath A, Dorababu N, Sirisha Mulukuri NVL, Sunil Kumar KT, Chandana SM, Chetty MC, Bendale AR, Rudrapal M (2022b) In vivo immunomodulatory activity and in silico study of *Albizia procera* bark extract on doxorubicin induced immunosuppressive rats. Journal of King Saud University-Science 34(3): 101828. https://doi.org/10.1016/j.jksus.2022.101828

Pasala PK, Uppara RK, Rudrapal M, Zothantluanga JH, Umar AK (2022a) Silybin phytosomes attenuates cerebral ischemia-reperfusion injury in rats by suppressing oxidative stress and reducing inflammatory response: *In vivo* and *in silico* approaches. Journal of Biochemical and Molecular Toxicology 36(7): e23072. https://doi.org/10.1002/jbt.23073

Issahaku AR, Salifu EY, Agoni C, Alahmdi MI, Abo-Dya NE, Soliman ME, Rudrapal M, Podila N (2023) Discovery of potential KRAS-SOS1 inhibitors from South African natural compounds: An *in silico* approach. ChemistrySelect 8(24): e202300277. https://doi.org/10.1002/slct.202300277

Mollinedo F, Gajate C (2003) Microtubules, microtubule interfering agents and apoptosis. Apoptosis 8: 413–450. https://doi.org/10.1023/A:1025513106330

Naresh P, Pattanaik P, Priyadarshini RL, Reddy DR (2013) Synthetic characterization & antimicrobial screening of some novel 6-fluorobenzothiazole substituted [1,2,4] triazole analogues. International Journal of Pharma Research and Health Sciences 1(1): 18–25.

Naresh P, Shyam Sundar P, Pradheesh SJ, Shanthoshivan AG, Akashwaran S, Swaroop AK, Jubie S (2021) Drug repurposing of Daclatasvir and Famciclovir as antivirals against dengue virus infection by in silico and in vitro techniques. Indian Journal of Biochemistry and Biophysics 58(6): 557–564.

Nitin M, Jyoti A, Dheeraj A, Pankaj M, Tanaji M, Sivakumar T (2010) Synthesis, antimicrobial and anti-inflammatory activity of some 5-substituted-3-pyridine-1, 2, 4-triazoles. International Journal of PharmTech Research 2(4): 2450–2455.

Pathak N, Rathi E, Kumar N, Kini SG, Rao CM (2020) A review on anticancer potentials of benzothiazole derivatives. Mini Reviews in Medicinal Chemistry 20(1): 12–23. https://doi.org/10.2174/1389557519666190617153213

Paul A, Zothantluanga JH, Rakshit G, Celik I, Rudrapal M, Zaman K (2023) Computational simulations reveal the synergistic action of phytochemicals of *Morus alba* to exert anti-Alzheimer activity via inhibition of acetylcholinesterase and glycogen synthase kinase-3 beta. Polycyclic Aromatic Compounds. https://doi.org/10.1080/10406638.2023.2236759

Prabhu PP, Panneerselvam T, Shastry CS, Sivakumar A, Pande SS (2015) Synthesis and anticancer evaluation of 2-phenyl thiaolidinone substituted 2-phenyl benzothiazole-6-carboxylic acid derivatives. Journal of Saudi Chemical Society 19(2): 181–185. https://doi.org/10.1016/j.jscs.2012.02.001

Raheel R, Saddiqe Z, Iram M, Afzal S (2017) *In vitro* antimitotic, antiproliferative and antioxidant activity of stem bark extracts of *Ficus benghalensis* L. South African Journal of Botany 111: 248–257. https://doi.org/10.1016/j.sajb.2017.03.037

Rajeeva B, Srinivasulu N, Shantakumar SM (2009) Synthesis and antimicrobial activity of some new 2-Substituted benzothiazole derivatives. Journal of Chemistry 6: 775–779. https://doi.org/10.1155/2009/404596

Rashid IA, Mukelabai N, Agoni C, Rudrapal M, Aldosari SM, Ibrahim I, Almalki SG, Khan J (2022) Characterization of the binding of MRTX1133 as an avenue for the discovery of potential KRASG12D inhibitors for cancer therapy. Scientific Reports 12(1): 17796. https://doi.org/10.1038/s41598-022-22668-1

Rudrapal M, Celik I, Chinnam S, Ansari MA, Khan J, Alghamdi S, Almehmadi M, Zothantluanga JH, Khairnar SJ (2022b) Phytocompounds of Indian spices as inhibitors of SARS-CoV-2 Mpro and PLpro: Molecular docking, molecular dynamics, and ADMET studies. Saudi Journal of Biological Sciences 29: 3456–3465. https://doi.org/10.1016/j.sjbs.2022.02.028

Rudrapal M, Celik I, Chinnam S, Çevik UA, Tallei TE, Nizam A, Joy F, Abdellattif MH, Walode SG (2022a) Analgesic and anti-inflammatory potential of indole derivatives. Polycyclic Aromatic Compounds. https://doi.org/10.1080/10406638.2022.2139733

Rudrapal M, Celik I, Khan J, Ismail RM, Ansari MA, Yadav R, Sharma T, Tallei TE, Pasala PK, Sahoo RK, Khairnar SJ, Bendale AR, Zothantluanga JH, Chetia D, Walode SG (2022c) Identification of bioactive molecules from Triphala (Ayurvedic herbal formulation) as potential inhibitors of SARS-CoV-2 main protease (Mpro) through computational investigations. Journal of King Saud University – Science 34(3): 101826. https://doi.org/10.1016/j.jksus.2022.101826

Rudrapal M, Gogoi N, Chetia D, Khan J, Banwas S, Alshehri B, Alaidarous MA, Laddha UD, Khairnar SJ, Walode SG (2022d) Repurposing of phytomedicine-derived bioactive compounds with promising anti-SARS-CoV-2 potential: Molecular docking, MD Simulations and Drug-Likeness/ ADMET Studies. Saudi Journal of Biological Sciences 29: 2432–2446. https://doi.org/10.1016/j.sjbs.2021.12.018

Rudrapal M, Eltayeb WA, Rakshit G, El-Arabey AA, Khan J, Aldosari SM, Alshehri B, Abdalla M (2023) Dual synergistic inhibition of COX and LOX by potential chemicals from Indian daily spices investigated through detailed computational studies. Scientific Reports 13(1): 8656. https://doi.org/10.1038/s41598-023-35161-0

Rudrapal M, Rashid IA, Agoni C, Bendale AR, Nagar A, Soliman MES, Lokwani D (2022e) *In silico* screening of phytopolyphenolics for the identification of bioactive compounds as novel protease inhibitors effective against SARS-CoV-2. Journal of Biomolecular Structure and Dynamics 40(20): 10437–10453. https://doi.org/10.1080/07391102.2021.1944909

Sharma PC, Sinhmar A, Sharma A, Rajak H, Pathak DP (2013) Medicinal significance of benzothiazole scaffold: an insight view. Journal of Enzyme Inhibition in Medicinal Chemistry 28(2): 240–266. https://doi.org/10.3109/14756366.2012.720572

Siddiqui N, Pandeya SN, Khan SA, Stables J, Rana A, Alam M, Arshad MF, Bhat MA (2007) Synthesis and anticonvulsant activity of sulfonamide derivatives-hydrophobic domain. Bioorganic and Medicinal Chemistry Letters 17(1): 255–259. https://doi.org/10.1016/j.bmcl.2006.09.053

Zothantluanga JH, Abdalla M, Rudrapal M, Tian Q, Chetia D, Li J (2022) Computational investigations for identification of bioactive molecules from *Baccaurea ramiflora* and *Bergenia ciliate* as inhibitors of SARS-CoV-2 Mpro. Polycyclic Aromatic Compounds 43(3): 2459–2487. https://doi.org/10.1080/10406638.2022.2046613